Six-Nucleon Spectroscopy from a Realistic Nonlocal Hamiltonian

P. Navrátil,[1,2] J. P. Vary,[3] W. E. Ormand,[1] and B. R. Barrett[4]

[1]*Lawrence Livermore National Laboratory, L-414, P.O. Box 808, Livermore, California 94551*
[2]*Nuclear Physics Institute, Academy of Sciences of the Czech Republic, 250 68 Řež near Prague, Czech Republic*
[3]*Department of Physics and Astronomy, Iowa State University, Ames, Iowa 50011*
[4]*Department of Physics, P.O. Box 210081, University of Arizona, Tucson, Arizona 85721*

(Received 11 May 2001; published 9 October 2001)

We apply the *ab initio* no-core nuclear shell model to solve the six-nucleon systems, ^{6}Li and ^{6}He, interacting by realistic nucleon-nucleon (*NN*) potentials. In particular, we present the first results for $A = 6$ with the nonlocal CD-Bonn *NN* potential. The resulting ^{6}Li binding energy $-29.3(6)$ MeV and the excitation spectra improve the agreement between the theory and experiment compared to results with local *NN* potentials, but the need for the inclusion of a real three-body interaction and/or further improvement of the *NN* forces remains. We predict properties of the ^{6}He dipole modes, a subject of current controversy.

DOI: 10.1103/PhysRevLett.87.172502 PACS numbers: 21.60.Cs, 21.10.Dr, 21.30.Fe, 27.20.+n

Various methods exist to solve $A \leq 4$ systems with realistic interactions [1–4]. Beyond $A = 4$, the Green's function Monte Carlo (GFMC) method is the only approach for which exact solutions of systems with $A \leq 8$ have been obtained thus far [4]. These results are generally obtained for local r-space potentials.

For both few-nucleon systems and the p-shell nuclei we apply the no-core shell model (NCSM) approach [5–7]. We have previously used this *ab initio* method to solve the $A = 3, 4$ bound-state problems [6], as well as the low-lying spectroscopy of ^{12}C [7]. Our approach is sufficiently flexible that we can treat nonlocal potentials, such as CD-Bonn [8]. We note that the CD-Bonn produces more accurate binding energy (BE) for $A = 3$ and $A = 4$ systems, while the local AV18 *NN* potential [4] seems to be more accurate in nuclear matter [9]. In this Letter, we present results for ^{6}Li and ^{6}He obtained with the nonlocal CD-Bonn *NN* potential achieving reasonable convergence in model spaces comprising up to 12 major harmonic oscillator (HO) shells. One of our goals is to achieve sufficient predictive power to shed light on the controversy over whether a soft dipole is present in ^{6}He [10,11]. We also remark that nonlocal potentials are likely to become more important as they are derived by effective-field theories based on QCD [12].

In the NCSM, we start from the intrinsic two-body Hamiltonian for the A-nucleon system $H_A = T_{\rm rel} + \mathcal{V}$, where $T_{\rm rel}$ is the relative kinetic energy and $\mathcal{V}$ is the sum of two-body nuclear and Coulomb interactions. Since we solve the many-body problem in a finite HO basis space, it is necessary that we derive a model-space dependent effective Hamiltonian. For this purpose, we perform a unitary transformation [6,7,13,14] of the Hamiltonian, which accommodates the short-range correlations. In general, the transformed Hamiltonian is an A-body operator. Our simplest, yet nontrivial, approximation is to develop a two-particle cluster effective Hamiltonian, while the next improvement is to include three-particle clusters, etc. The effective interaction is then obtained from the decoupling condition between the model space and the excluded space for the two-nucleon transformed Hamiltonian. The resulting two-body effective Hamiltonian depends on the nucleon number A, the HO frequency Ω, and $N_{\rm max}$, the maximum many-body HO excitation energy defining the model space. The effective interaction approaches the bare interaction for $N_{\rm max} \to \infty$.

To gauge convergence, we aim for independence of basis space parameters and compare with results of other methods. Our method is not variational so the neglected effects may contribute with either sign to total BE.

As a test case we solved the $A = 3$ and 4 systems employing a translationally invariant HO basis [6] with the semirealistic Minnesota (MN) [15] and MT-V [16] *NN* potentials, as well as the realistic potentials CD-Bonn [8], AV18, and AV8′ [4] (see Table I). For the $A = 3$ systems, we used basis spaces up to $50\hbar\Omega$ ($N_{\rm max} = 50$), while our $A = 4$ results were obtained in basis spaces up to $18\hbar\Omega$ using, for the most part, two-body effective interactions. For ^{4}He with AV8′ or AV18, this was insufficient, and for AV8′ we used the three-body effective interaction, which

TABLE I. NCSM results for the ground-state energies, in MeV, of ^{3}H, ^{3}He, and ^{4}He. Our estimated uncertainties in the last digit(s) are given in parentheses. The MT-V and the AV8′ calculations do not include the Coulomb interaction.

NN pot	MN	MT-V	CD-Bonn	AV8′	AV18
^{3}H	−8.385(2)	−8.239(4)	−8.002(4)	−7.75(2)	−7.61(1)
^{3}He			−7.249(4)		−6.90(1)
^{4}He	−29.94(1)	−31.28(8)	−26.30(15)	−25.80(20)	

 0031-9007/01/87(17)/172502(4)$15.00

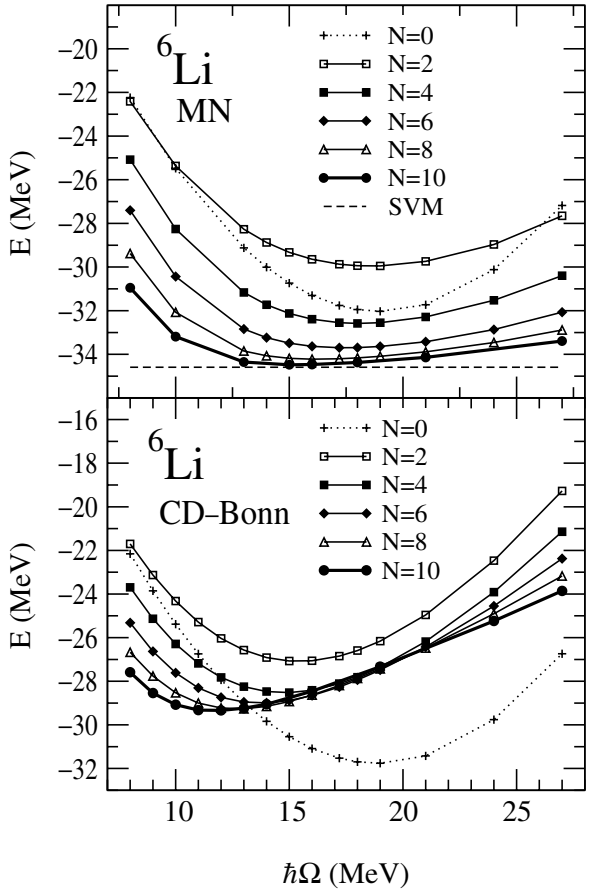

FIG. 1. Calculated ground-state energy of ^{6}Li using the MN potential (upper panel) and the CD-Bonn *NN* potential (lower panel). Results obtained in $0\hbar\Omega-10\hbar\Omega$ basis spaces in the range of HO frequencies of $\hbar\Omega = 8-27$ MeV are presented.

improved convergence. Overall, our $A = 3$ and $A = 4$ results are in excellent agreement with other exact methods, as is exhibited in the comparison in Table I with results presented in Refs. [15,17] and references therein.

To solve for the properties of ^{6}Li and ^{6}He, we employ the *m*-scheme many-fermion dynamics code [18]. At present our calculations are limited to $N_{\max} \leq 10$ where the basis dimension reaches 9 692 634.

We test our method for $A = 6$ using the semirealistic MN potential. In the upper panel of Fig. 1, we show the frequency dependence of the ^{6}Li ground state from $\hbar\Omega = 8-27$ MeV. Starting from the $2\hbar\Omega$ space we find a uniform behavior and achieve reasonable convergence at $10\hbar\Omega$. The BE in the flat region around $\hbar\Omega = 15$ MeV reaches $-34.48(26)$ MeV, with the uncertainty estimated as the difference from the $8\hbar\Omega$ result. This result agrees well with -34.59 MeV obtained with the stochastic variational method (SVM) [15].

In the lower panel of Fig. 1, we present the results using the CD-Bonn *NN* potential including Coulomb. Here, the trends are more complex. The flat regions still expand and converge but shift to lower frequency with increasing $N_{\max}$. The overall frequency dependence is stronger than found with the MN potential. The trends of our ^{6}Li MN and ^{4}He results support taking our best result from the largest model space in the region with minimal dependence on the HO frequency. Thus, our best result for ^{6}Li with CD-Bonn is for $\hbar\Omega \approx 12-13$ MeV, i.e., BE $= -29.34$ MeV.

TABLE II. NCSM, GFMC, and SVM results for the ^{6}Li ground-state energies and point-proton rms radii, excitation energies, and quadrupole and magnetic moments using the MN, AV8′, and CD-Bonn *NN* potentials. The AV8′ results do not include the Coulomb interaction. The NCSM ground-state energies in the upper part are deduced from the investigation of least dependence on HO frequency. In the lower part of the table we show the ^{6}Li $10\hbar\Omega$ NCSM results obtained with $\hbar\Omega = 13$ MeV. The $r_{\mathrm{gs},p}$ uncertainty is estimated from its HO frequency and basis size dependence. The experimental values are from Ref. [20].

^{6}Li $E_{\mathrm{gs}}(1^+0)$ [MeV]	NCSM	Comparison
MN	$-34.48(26)$	-34.59 (SVM)
AV8′	-30.30	$-29.70(5)$ (GFMC)
CD-Bonn	$-29.34(60)$	-31.995 (Expt)

^{6}Li	GFMC AV8′	NCSM AV8′	NCSM CD-Bonn	Expt
$r_{\mathrm{gs},p}$ [fm]	2.50(1)	$2.16(^{+25}_{-9})$	$2.16(^{+25}_{-9})$	2.32(3)
Q_{gs} [e fm^2]	$-0.27(8)$	-0.069	-0.042	-0.083
μ_{gs} [μ_N]	$+0.823(1)$	$+0.845$	$+0.847$	$+0.822$
$E_x(3^+0)$ [MeV]	3.21(7)	2.909	2.841	2.186
$E_x(0^+1)$ [MeV]	3.94(8)	3.526	3.330	3.563
$E_x(2^+0)$ [MeV]	4.10(6)	4.490	4.610	4.310
$E_x(2^+_1 1)$ [MeV]	5.98(8)	6.039	5.975	5.366
$E_x(1^+_2 0)$ [MeV]		6.479	6.544	5.65
$E_x(2^+_2 1)$ [MeV]		9.216	9.199	
$E_x(1^+1)$ [MeV]		9.895	9.937	

To obtain a realistic estimate of the uncertainty in our BE, we solved ^{6}Li using the AV8′ *NN* potential without Coulomb, where the solution, $-29.70(5)$ MeV, is known

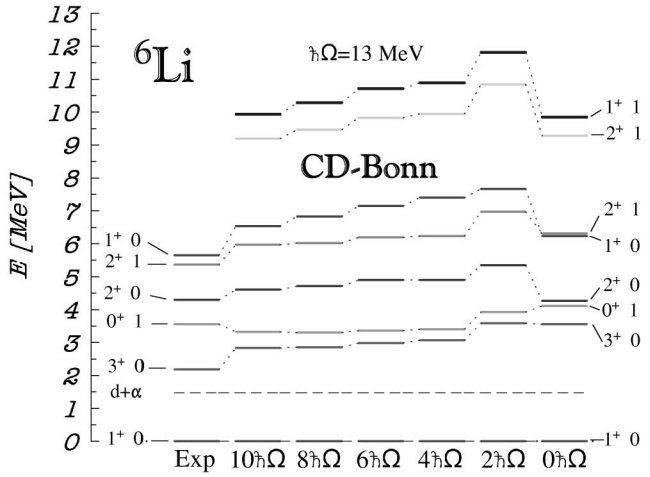

FIG. 2. Experimental and theoretical positive-parity excitation spectra of ^{6}Li. Results obtained in $0\hbar\Omega-10\hbar\Omega$ basis spaces using the CD-Bonn *NN* potential with $\hbar\Omega = 13$ MeV are presented. The experimental values are from Ref. [20].

TABLE III. The NCSM ^{6}Li $E2$ transitions, in e^2 fm^4, and the ^{6}He ground-state and excitation energies, in MeV, point-nucleon rms radii, in fm, $E2$ transitions, in e^2 fm^4, $E1$ transitions, in e^2 fm^2 obtained using the CD-Bonn NN potential and the HO frequency $\hbar\Omega = 13$ MeV in the $6\hbar\Omega - 10\hbar\Omega$ basis spaces. The Gamow-Teller (GT) transitions were obtained in the $8\hbar\Omega$ space. The negative-parity excitation energies are relative to the corresponding 1_1^-1 state. The experimental values are from Ref. [20].

^{6}Li	$6\hbar\Omega$	$8\hbar\Omega$	$10\hbar\Omega$	Expt
$B(E2; 1^+0 \to 3^+0)$	8.166	9.136	10.221	21.8(4.8)
$B(M1; 0^+1 \to 1^+0)$	15.510	15.351	15.186	15.42(32)
$B(E2; 2^+0 \to 1^+0)$	3.414	3.989	4.502	4.41(2.27)
$B(M1; 2^+1 \to 1^+0)$	0.034	0.041	0.037	0.150(27)
^{6}He	$6\hbar\Omega$	$8\hbar\Omega$	$10\hbar\Omega$	Expt
$E_{gs}(0^+1)$	−26.414	−26.764	−26.709	−29.269
$r_{gs,p}$	1.747	1.754	1.763	1.72(4)
$r_{gs,n}$	2.281	2.323	2.361	2.59(4)
$E_x(2_1^+1)$	2.712	2.596	2.529	1.80
$E_x(2_2^+1)$	6.359	6.057	5.786	
$E_x(1^+1)$	7.204	6.848	6.504	
$E_x(0_2^+1)$	9.809	9.170	8.539	
$B(E2; 0^+ \to 2_1^+)$	0.735	0.889	1.056	
$B(E2; 0^+ \to 2_2^+)$	0.151	0.188	0.222	
^{6}He	$5\hbar\Omega$	$7\hbar\Omega$	$9\hbar\Omega$	
$E(1_1^-1)$	−16.463	−18.209	−19.269	
$E_x(2_1^-1)$	0.823	1.011	0.939	
$E_x(1_2^-1)$	3.783	3.553	3.296	
$E_x(0_1^-1)$	3.604	3.700	3.528	
$E_x(4_1^-1)$	5.567	5.501	5.161	
$E_x(1_3^-1)$	6.251	5.887	5.449	
$E_x(2_2^-1)$	6.533	6.245	5.824	
$E_x(3_1^-1)$	7.438	6.860	6.336	
$E_x(1_4^-1)$	9.284	8.201	7.470	
$E_x(1_5^-1)$	10.775	10.386	9.586	
$E_x(1_6^-1)$	12.293	11.420	11.250	
	$4\hbar\Omega \to 5\hbar\Omega$	$6\hbar\Omega \to 7\hbar\Omega$	$8\hbar\Omega \to 9\hbar\Omega$	
$B(E1; 0^+ \to 1_1^-)$	0.308	0.353	0.388	
$B(E1; 0^+ \to 1_2^-)$	0.080	0.083	0.089	
$B(E1; 0^+ \to 1_3^-)$	0.394	0.319	0.324	
$B(E1; 0^+ \to 1_4^-)$	0.0005	0.0004	0.0006	
$B(E1; 0^+ \to 1_5^-)$	0.0015	0.0000	0.0000	
$B(E1; 0^+ \to 1_6^-)$	0.0012	0.0007	0.0003	
^{6}Li → ^{6}He	CD-Bonn $\frac{\hbar\Omega=13\text{ MeV}}{\text{NCSM}}$		Expt	
$B(GT; 1^+0 \to 0_1^+1)$	1.770		1.576(5)	
$B(GT; 1^+0 \to 2_1^+1)$	0.001			
$B(GT; 1^+0 \to 2_2^+1)$	0.055			
$B(GT; 1^+0 \to 1^+1)$	0.027			
$B(GT; 1^+0 \to 0_2^+1)$	0.048			

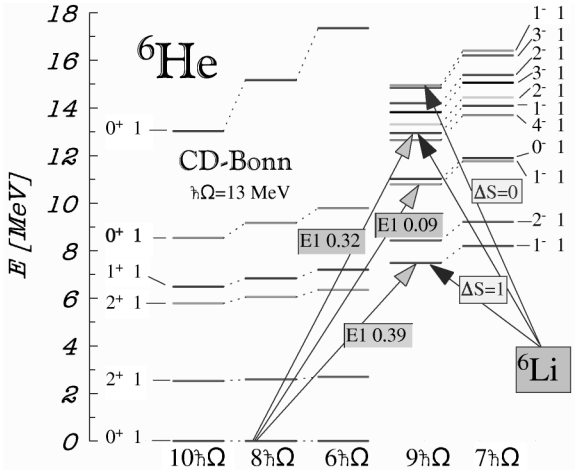

FIG. 3. Positive- and negative-parity excitation spectra of ^{6}He. Results obtained in $7\hbar\Omega - 10\hbar\Omega$ basis spaces using the CD-Bonn NN potential with $\hbar\Omega = 13$ MeV are presented. The $7(9)\hbar\Omega$ excitation energies are relative to the $6(8)\hbar\Omega$ ground state. The arrows indicate strong $E1$ and charge transfer transitions. See text and Tables III and IV for details.

from the GFMC method [4,19]. As for ^{4}He, we obtain a stronger frequency dependence for AV8′ than for CD-Bonn indicating slower convergence. Our $10\hbar\Omega$ ^{6}Li result for AV8′ (no Coulomb) gives a BE of −30.30 MeV. We use this and the above GFMC result to infer a conservative estimate of the uncertainty in our CD-Bonn ground-state energy; i.e., we quote BE = −29.34(60) MeV.

We note that CD-Bonn provides significantly more BE for ^{6}Li than does AV18, −26.89(10) MeV [4,19]. Yet, the experimental value is −31.995 MeV [20], so CD-Bonn underbinds (upper part of Table II) by about the same amount as it underbinds ^{4}He (Table I).

In Fig. 2, we compare our calculated ^{6}Li excitation spectra obtained using the CD-Bonn NN potential in model spaces from $0\hbar\Omega$ to $10\hbar\Omega$ with experiment. In Table II, we also show our $10\hbar\Omega$ levels obtained using the AV8′ together with the GFMC results [19]. Here, we utilize $\hbar\Omega = 13$ MeV which lies in the range where the largest basis space yields results least sensitive to $\hbar\Omega$, as seen in Fig. 1 for the CD-Bonn case. We note that the CD-Bonn spectrum, as well as the AV8′ spectrum, exhibits good stability for the low-lying states for $N_{\max} \geq 4$. The higher lying states are broad resonances so their movement is not unexpected. Although the level ordering is excellent, we see that the calculated spectrum does not fully agree with experiment. The theoretical 3^+0 state is too high and the splitting between the 2^+0 and 3^+0 states is smaller than observed. On the other hand, we obtain reasonable agreement between our AV8′ excitation spectra with that obtained with GFMC. Consequently, we conclude that the CD-Bonn NN potential cannot by itself reproduce the low-lying experimental spectrum of ^{6}Li. However, CD-Bonn is a slight improvement over the Argonne potentials, in that the 3^+0 state is lower and the spin-orbit splitting between the 2^+0 and 3^+0 states is larger. We note, though, that our calculation produces a larger spin-orbit splitting for the AV8′ than the GFMC calculation does. This could perhaps be attributed to an incomplete convergence of the 2^+0 state with increasing basis space.

TABLE IV. The NCSM $^6\mathrm{Li} \rightarrow {}^6\mathrm{He}$ representative charge transfer matrix elements squared and divided by $2J_i + 1$. See the text for details.

$^6\mathrm{Li} \rightarrow {}^6\mathrm{He}$	$\Delta S = 0$	$(\Delta S = 1)^{(0)}$	$(\Delta S = 1)^{(1)}$	$(\Delta S = 1)^{(2)}$
$1^+0 \rightarrow 1_1^-1$	0.024	0.157	0.287	0.329
$1^+0 \rightarrow 1_2^-1$	0.061	0.0004	0.009	0.347
$1^+0 \rightarrow 1_3^-1$	0.009	0.043	0.207	0.406
$1^+0 \rightarrow 1_4^-1$	0.294	0.181	0.056	0.081
$1^+0 \rightarrow 1_5^-1$	0.004	0.083	0.034	0.009
$1^+0 \rightarrow 1_6^-1$	0.083	0.069	0.053	0.106

In Table III, we present results for electromagnetic transitions for ^{6}Li and ^{6}He obtained using $\hbar\Omega = 13$ MeV in basis spaces from $6\hbar\Omega$ to $10\hbar\Omega$. We see that the $E2$ transitions are not converged and that the use of effective operators, as discussed in Ref. [7], is necessary and will be done in the future. Similarly, our point-nucleon rms radii increase with the basis size for both ^{6}Li and ^{6}He. On the other hand, the $M1$, $E1$, and the Gamow-Teller transitions show better stability and agree reasonably well with experiment. This gives us confidence to address the question of soft-dipole modes in ^{6}He.

Recently, a charge exchange (^{7}Li, ^{7}Be) reaction on ^{6}Li showed evidence of a soft-dipole mode in ^{6}He [10]. In particular, a strong $\Delta L = 1$ spin-flip transition was found concentrated at about 4 MeV of excitation in ^{6}He, while the $\Delta L = 1$ spin-nonflip transition excited a giant dipole resonance analog state at about 8.5 MeV. Similarly, in the $(t, {}^3\mathrm{He})$ reaction, a broad asymmetric structure at $E_x \approx 5$ MeV dominated by dipole states was reported in Ref. [11]. We find very strong $E1$ transitions from the ^{6}He ground state to the 1_1^-1 and 1_3^-1 states (Table III and Fig. 3). In order to discuss $\Delta L = 1$ charge transfer strength from ^{6}Li to ^{6}He including spin selectivity, we introduce the operators $rY_1 t_-$ ($\Delta S = 0$) and $(rY_1\sigma)^{(K)} t_-$ ($\Delta S = 1$). Our results, obtained using the $8\hbar\Omega \rightarrow 9\hbar\Omega$ basis, are tabulated in Table IV and schematically shown in Fig. 3. We observe that the $\Delta S = 1$ charge transfer transition is mostly divided between the 1_1^-1 and 1_3^-1 states, which are separated by about 5.5 MeV. On the other hand, the $\Delta S = 0$ charge transfer transition is concentrated in the 1_4^-1 state, which is a couple of MeV higher in excitation energy. This complex behavior of the dipole states is consistent with experiment if these levels are shifted a few MeV lower in the excitation spectrum. It is very reasonable to expect such a shift as the overall trend of the dipole states is to decrease in excitation energy with increasing $N_{\max}$ (Table III and Fig. 3), which contrasts with, e.g., the 2_1^+1 state stability and suggests that the negative-parity states are rather broad resonances. Consequently, our results tend to support the soft-dipole mode interpretation of the experimental observations in Ref. [10].

This work was performed in part under the auspices of the U.S. Department of Energy by the University of California, Lawrence Livermore National Laboratory under Contract No. W-7405-Eng-48. This work was supported in part from LDRD Contract No. 00-ERD-028, by NSF Grant No. PHY0070858, and by USDOE Grant No. DE-FG-02-87ER-40371, Division of High Energy and Nuclear Physics.

[1] L. D. Faddeev, Sov. Phys. JETP **12**, 1014 (1961); J. L. Friar, G. L. Payne, V. G. J. Stoks, and J. J. de Swart, Phys. Lett. B **311**, 4 (1993).
[2] O. A. Yakubovsky, Sov. J. Nucl. Phys. **5**, 937 (1967); W. Glöckle and H. Kamada, Phys. Rev. Lett. **71**, 971 (1993).
[3] M. Viviani, A. Kievsky, and S. Rosati, Few-Body Syst. **18**, 25 (1995).
[4] B. S. Pudliner *et al.,* Phys. Rev. C **56**, 1720 (1997); R. B. Wiringa, Nucl. Phys. **A631**, 70c (1998); R. B. Wiringa, S. C. Pieper, J. Carlson, and V. R. Pandharipande, Phys. Rev. C **62**, 014001 (2000); S. C. Pieper, V. R. Pandharipande, R. B. Wiringa, and J. Carlson, Phys. Rev. C **64**, 014001 (2001).
[5] D. C. Zheng *et al.,* Phys. Rev. C **48**, 1083 (1993); D. C. Zheng, J. P. Vary, and B. R. Barrett, Phys. Rev. C **50**, 2841 (1994); D. C. Zheng *et al.,* Phys. Rev. C **52**, 2488 (1995); P. Navrátil and B. R. Barrett, Phys. Rev. C **54**, 2986 (1996); Phys. Rev. C **57**, 3119 (1998).
[6] P. Navrátil and B. R. Barrett, Phys. Rev. C **57**, 562 (1998); **59**, 1906 (1999); P. Navrátil, G. P. Kamuntavičius, and B. R. Barrett, Phys. Rev. C **61**, 044001 (2000).
[7] P. Navrátil, J. P. Vary, and B. R. Barrett, Phys. Rev. Lett. **84**, 5728 (2000); Phys. Rev. C **62**, 054311 (2000).
[8] R. Machleidt, F. Sammarruca, and Y. Song, Phys. Rev. C **53**, 1483 (1996).
[9] L. Engvik *et al.,* Nucl. Phys. **A627**, 85 (1997).
[10] S. Nakayama *et al.,* Phys. Rev. Lett. **85**, 262 (2000).
[11] T. Nakamura *et al.,* Phys. Lett. B **493**, 209 (2000).
[12] U. van Kolck, Phys. Rev. C **49**, 2932 (1994); E. Epelbaum *et al.,* e-print nucl-th/0007057.
[13] K. Suzuki and S. Y. Lee, Prog. Theor. Phys. **64**, 2091 (1980); K. Suzuki, Prog. Theor. Phys. **68**, 246 (1982); **68**, 1999 (1982); K. Suzuki and R. Okamoto, Prog. Theor. Phys. **92**, 1045 (1994).
[14] J. Da Providencia and C. M. Shakin, Ann. Phys. (N.Y.) **30**, 95 (1964); E. M. Krenciglowa and T. T. S. Kuo, Nucl. Phys. **A235**, 171 (1974).
[15] K. Varga and Y. Suzuki, Phys. Rev. C **52**, 2885 (1995).
[16] R. A. Malfliet and J. A. Tjon, Nucl. Phys. **A127**, 161 (1969).
[17] A. Nogga, H. Kamada, and W. Glöckle, Phys. Rev. Lett. **85**, 944 (2000); N. Barnea, W. Leidemann, and G. Orlandini, Phys. Rev. C **61**, 054001 (2000).
[18] J. P. Vary, "The Many-Fermion-Dynamics Shell-Model Code," Iowa State University, 1992 (unpublished); J. P. Vary and D. C. Zheng, *ibid.,* 1994.
[19] S. C. Pieper (private communication).
[20] F. Ajzenberg-Selove, Nucl. Phys. **A490**, 1 (1988); I. Tanihata *et al.,* Phys. Lett. B **206**, 592 (1988); **289**, 261 (1992); G. D. Alkhazov *et al.,* Phys. Rev. Lett. **78**, 2313 (1997).